ARCHIVES OF METALLURGY

Volume 45 2000 Issue 2

JOSE C. ESCOBEDO BOCARDO*, MARCO A. RAMIREZ A.*,
JANUSZ DONIZAK**, ZYGMUNT KOLENDA**

COMPUTER-AIDED COOLING CURVE ANALYSIS APPLIED TO Co–Cr–Mo SYSTEM

ANALIZA NUMERYCZNA KRZYWEJ STUDZENIA W ZASTOSOWANIU DO BADANIA KRZEPNIĘCIA STOPU Co–Cr–Mo

Computer-aided cooling curve analysis has been applied to a cobalt-based alloy, (widely used in the production of surgical implants) resulting in better understanding of the solidification process. Transformation temperatures and latent heat of solidification have been evaluated. Further kinetics study of solidification has been made yielding information on the evolution of solid fraction during solidification process. Segregation patterns were obtained by means of metallographic and microanalysis techniques.

Numeryczna analiza krzywej studzenia próbki stopu Co–Cr–Mo pozwoliła na dokonanie badań, które na ogół wykonuje się w klasycznej analizie termicznej przy wykorzystaniu wysoce specjalistycznego sprzętu. Poza czynnikiem ekonomicznym o sposobie wykonania analizy zadecydowała także wysoka temperatura krzepnięcia badanego stopu, która utrudnia wykonanie klasycznej analizy termicznej. W trakcie badań określono temperatury charakteryzujące przebieg zjawiska krzepnięcia tego stopu, wyznaczono także ciepło utajone krzepnięcia. Kinetykę krzepnięcia ujęto w formie relacji ułamka fazy stałej w funkcji czasu przebiegu procesu krzepnięcia. Zjawiska segregacji opisano dzięki zastosowaniu badań metalograficznych oraz mikroanalizy.

* CENTRO DE INVESTIGACIÓN Y DE ESTUDIOS AVANZADOS DEL IPN, SALTILLO COAHUILA, MEXICO
** KATEDRA TEORII I INŻYNIERII PROCESÓW METALURGICZNYCH, AKADEMIA GÓRNICZO-HUTNICZA, 30-059 KRAKÓW, AL. MICKIEWICZA 30

1. Introduction

Instrumental thermal analysis has been proved to be a powerful tool in the quality control of many commercial alloys. Several techniques, including derivative thermal analysis, differential thermal analysis [1, 2], and temperature difference thermal analysis [3, 4], have been developed. The set of the above techniques gives information about grain size, structural modifications, size and nature of the many precipitated phases that can be observed in multicomponent commercial systems.

However, the results of thermal analysis, metallographic and microanalysis techniques should be necessarily combined together in order to obtain deeper understanding of crystallization processes. Derivative thermal analysis and temperature difference thermal analysis are performed using appropriate mathematical and numerical methods to interpret the cooling curve data collected from experimental investigations.

The classical differential thermal analysis provides complete and precise information about the heat evolution of sample during its phase transformation, but investigation must be performed under strictly controlled laboratory experimental conditions using relatively expensive equipment with difficulties to operate at high temperature.

Due to the inconveniences of applying the traditional differential thermal analysis equipment in the foundry environment, the computer-aided cooling curve analysis can be used to simulate the classical method, using simple, cheap and mobile data acquisition microcomputer system [5, 7]. The low cost and versatility of this method, in spite of the lower precision compared with classical differential thermal analysis (but still at acceptable level of confidence), make it an attractive method for thermal analysis.

In the presented work, computer-aided cooling curve analysis, metallographic and microanalysis techniques have been used to study the solidification process of the cobalt-based alloy.

2. Theoretical background

2.1. Computer-aided cooling curve analysis

In classical differential thermal analysis the heat release due to the phase transformation is evaluated utilizing difference between temperature changes with time, measured instantaneously, in the metallic sample and in the neutral reference material. The same principle can be applied in analysis of the cooling. The "zero curve" (reference material) can be generated using the portion of the cooling curve without phase transformation, assuming constant cooling rate along the process. The area between the derivative of the sample cooling and zero

curves represents the amount of heat released or absorbed during the phase transformation. This area can be evaluated by numerical integration procedure [5–7].

From the heat balance equation of the sample, assuming Newtonian cooling, dumped system approximation and no phase change, the first derivative of the cooling becomes:

$$\frac{dT}{dt} = \left(\frac{hA}{V\varrho c_p}\right)(T - T_0), \tag{1}$$

where:

V — volume of the sample (m^3),
ϱ — density of the sample (kg m^{-3}),
c_p — specific heat of the sample material (J kg^{-1} K^{-1}),
t — time (sec),
$T(t)$ — temperature of the sample (K),
h — heat transfer coefficient (W m^{-2} K^{-1}),
T_0 — ambient temperature (K).

Eq. (1) represents reference "zero curve".

Assuming constant properties of the sample material and using mean value for heat transfer coefficient, the solution of Eq. (1) takes the form:

$$T(t) = T_0 + (T_M - T_0)\exp(-Ct). \tag{2}$$

Applying initial condition

$$T(t = 0) = T_M$$

where T_M represents pouring temperature, (K), constant value

$$C = \left(\frac{hA}{V\varrho c_p}\right).$$

Combining solution (2) with Eq. (1), reference cooling curve is described by:

$$\frac{dT}{dt} = (T_M - T_0)\,C\exp(-Ct). \tag{3}$$

Under the same assumption, considering that phase change occurs during sample cooling, derivative of the real cooling curve of the metallic sample during solidification, i.e. when solidification effects are included, can be expressed in the form

$$\frac{dT}{dt} = \left(\frac{1}{V\varrho c_p}\right)\left[hA(T - T_0) - \frac{dQ_L}{dt}\right] \tag{4}$$

where:

$\frac{dQ_L}{dt}$ represents the rate of heat released due to the phase transformation (W).

Subtracting Eq. (3) from Eq. (4) and integrating, the heat released during solidification per unit mass becomes:

$$\frac{Q_L}{V\varrho} = -c_p\left[\int_0^t \left(\frac{dT}{dt}\right)_{cc} dt - \int_0^t \left(\frac{dT}{dt}\right)_{zc} dt\right], \tag{5}$$

where $\left(\frac{dT}{dt}\right)_{cc}$ and $\left(\frac{dT}{dt}\right)_{zc}$ represent real cooling curve and zero curve (reference curve) respectively.

If the integration time interval covers whole solidification period, numerical values obtained from Eq. (5) represent latent heat of solidification L, (J kg^{-1}), of the sample.

2.2. Solidification kinetics

Assuming that latent heat of solidifying phase L, is by definition constant value, the rate of heat evolution due to the phase transformation can be expressed in term of solid fraction rate change

$$-\frac{dQ_L}{dt} = \varrho V L \frac{df_s}{dt}. \tag{7}$$

Combining Eq. (4) with Eq. (5) and Eq. (7) and after integrating over time expression relating solid fraction evolution with time occurs in the form, [3]:

$$f_s(\tau) = \frac{c_p}{L}\left[\int_0^\tau \left(\frac{dT}{dt}\right)_{cc} dt - \int_0^\tau \left(\frac{dT}{dt}\right)_{zc} dt\right]. \tag{8}$$

If the latent heat of solidification and the specific heat capacity of solid and liquid are known, recorded temperature history of the sample (in the form of cooling curve) allows evaluation of the time dependent solid fraction evolution $f_s(\tau)$.

3. Experimental procedure

Chemical analyses of the selected alloys under investigation are presented in table 1.

TABLE 1

Chemical composition of selected alloys

Element (wt.%)	Sample 1	Sample 2, 3 and 4
C	0.23	0.22
Mn	0.42	0.38
Si	0.66	0.82
Ni	0.71	0.36
Cr	26.02	25.75
Mo	6.11	5.74
Fe	0.95	0.38
W	0.23	0.07
Co	66.19	64.60

3.1. Sample preparation

About 3 kg of alloy was melted under an inert atmosphere of argon in a vacuum induction furnace equipped with alumina crucible. The melt was heated up to 1600°C. Alloy samples were poured into small, alumina crucibles that were preheated to 1200°C.

Thermocouples (type R), fixed to the alumina crucible cap, were immediately dipped after pouring into the melt. The tips of thermocouples were located 15 mm above the bottom of the crucible and centered in the sample. Thermocouple wires were connected to the solid panel (terminal Panel T11, Strawberry Tree Inc.) equipped with an isothermal plate for accurate temperature measurements. Data acquisition and control card installed in the microcomputer collected data from terminal panel at constant frequency (0.1 sec). The linearisation procedure and cold junction compensation of the signal were handled automatically by the data acquisition board. Programming the data acquisition board and the measured data storage were performed using Workbench PC Data Acquisition and Control Software. Data were acquired and stored with accuracy of 0.1°C. For each particular alloy composition and cooling rate, the experiment was repeated at least three times for assuring reproducibility.

For metallographic examinations, the solidified samples were sectioned transversally, about 14 mm from bottom of the sample, ground and polished. An etching solution (50 ml HCl, 10 ml H_2O_2) was used to visualize grain boundaries. The identification and qualification of the phases were made using image analysis system, and the microanalysis was made using Energy Dispersive Spectrometry (EDS) and Scanning Electron Microscopy (SEM).

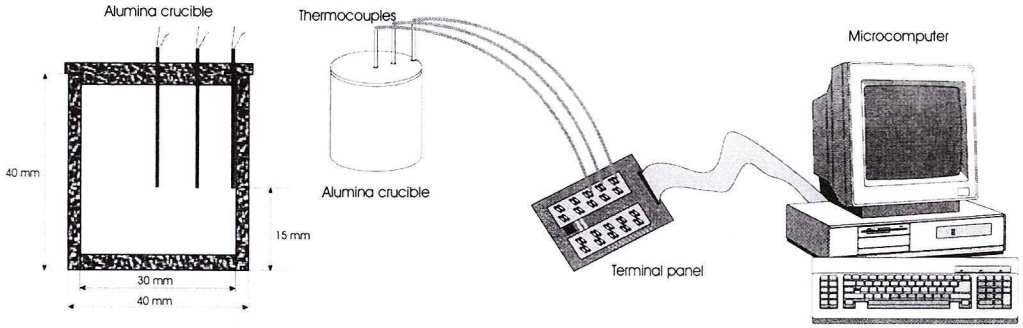

Fig. 1. Schematic representation of the experimental setup used in this work

4. Results and discussion

4.1. Determination of cooling curve characteristic points

Cooling curves recorded during experiment were smoothed using Fourier series [8] and their derivatives were calculated numerically point by point using the Savitsky-Golay algorithm [9]. The example of the smoothed cooling curve ant its first and second derivative for sample 1 (see table 1) is presented in figure 2.

In the Co–Cr–Mo alloys, the sequence of solidification, registered by thermal analysis, starts with the growing of equiaxed dendrites of primary phase (α phase), which is a solid solution rich in cobalt [10, 11]. When the primary dendrite tips

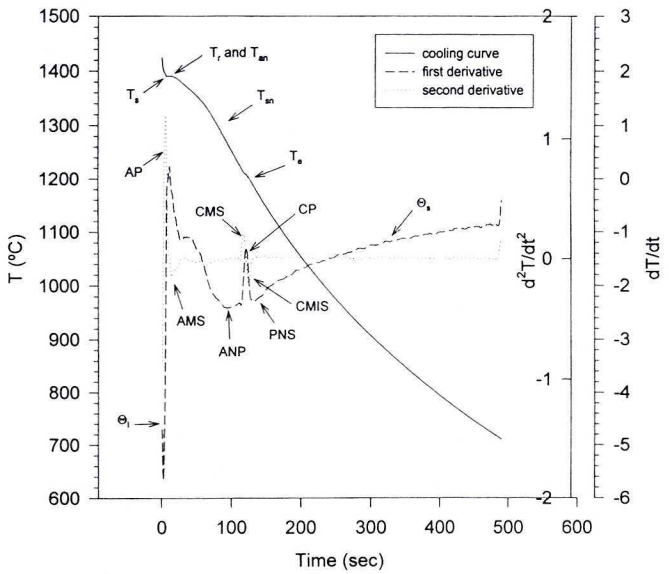

Fig. 2. Cooling curve and the first and second derivative of this curve as function of time

finish growing, the secondary and tertiary dendrite arms start to thicken [12, 14]. During these stages, a continuous solute segregation from the solid occurs, enriching the remnant liquid. When the temperature reaches approximately 1210°C and enough solute in the remnant liquid is present, a new interdendritic phase appears (carbides phase) and the solidification process ends. Then the cooling of the solid alloy begins. As it can be seen in Fig. 2, all the mentioned phenomena occuring during solidification process are registered in the form of cooling curve and its derivatives. The measured average characteristic points for the alloy are shown in table 2.

TABLE 2

Characteristic points

Characteristic point	Physical meaning	Temperature (°C)
Cooling curve		
T_s	Maximum super-cooling temperature (primary phase)	1387.31
T_r	Recalescence temperature during dendritic growing	1390
T_{an}	Nucleation temperature (primary phase)	1390
T_{sn}	Nucleation temperature (carbides phase)	1288.88
T_e	End of solidification temperaure	1191.34
First derivative		
AP	α phase peak. The area under the peak is proportional to the α phase content	1385.93
ANP	Negative α phase peak. End of α phase formation	1288.91
CP	Carbides peak. The area under the peak is proportional to the carbides phase content	1211.73
NCP	Negative carbides peak. End of carbides phase formation	1188.03
Θ_l	Average slope of the first derivative (cooling of liquid)	4.9e-3 (s^{-1})
Θ_s	Average slope of te first derivative (cooling of solid)	3.6e-3 (s^{-1})
Second derivative		
AMS	Minimum slope during α phase formation	1384.21
CMS	Maximum slope during carbides phase formation	1237.34
CMIS	Minimum slope during carbides phase formation	1193.34

4.2. Determination of the latent heat

Figures 3 and 4 illustrate the method used to calculate the latent heat of solidification for sample 2 (see table 1 for identification). The base line in Fig. 3 was

generated using Eq. (3), the difference between measured and base line is shown in Fig. 4. The peaks from the primary phase α and from the carbide phase are well defined and separated. The values of the latent heat of solidification were calculated

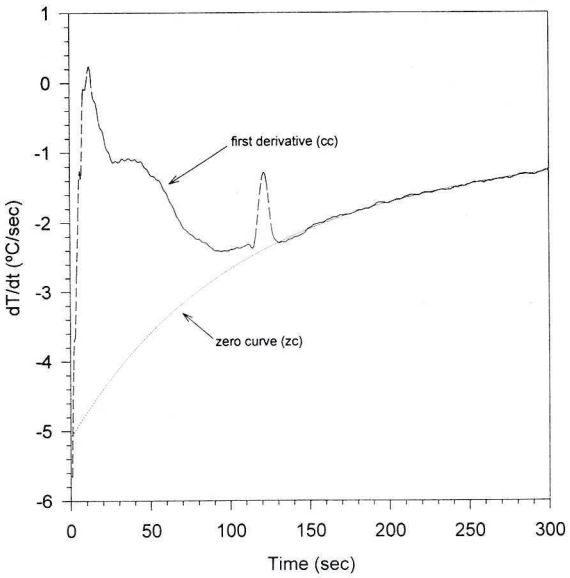

Fig. 3. First derivative as a function of time and base line

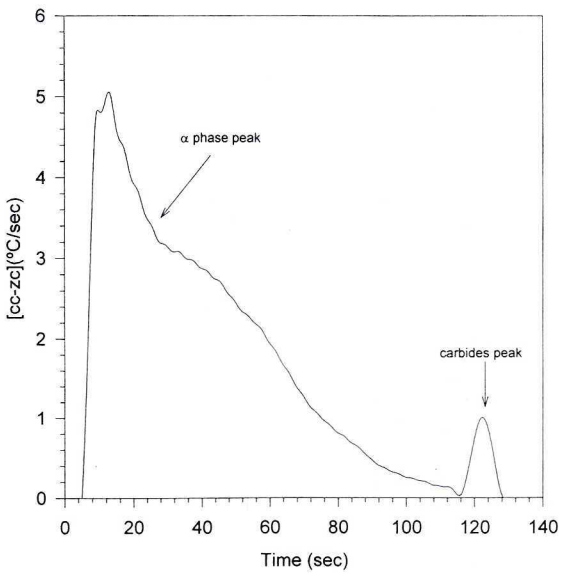

Fig. 4. First derivative as a function of time and base line in normalised form

from Eq. (5) and the phase percentages were obtained from the surface areas under the respective peaks in Fig. 4. Table 3 shows numerical values for selected alloy compositions.

TABLE 3

Latent heat of solidification and phase percent values for samples 2, 3 and 4

Sample	L (kJ kg^{-1})			Primary phase α (%)	Carbides phase (%)
	total	α phase	carbides phase		
2	183	176.3	6.7	96.34	3.66
3	195.48	188.97	6.51	96.67	3.33
4	205.69	198.49	7.2	96.5	3.5
Average	194.72	187.92	6.8	96.5	3.5

4.3. Solidification kinetics

Acquired data were used to estimate solid fraction evolution using Eq. (7), where previously calculated latent heat and reference curves were utilized. The resulting dependence of solid fraction vs. time is shown in Fig. 5, which corresponds to the data from table 2.

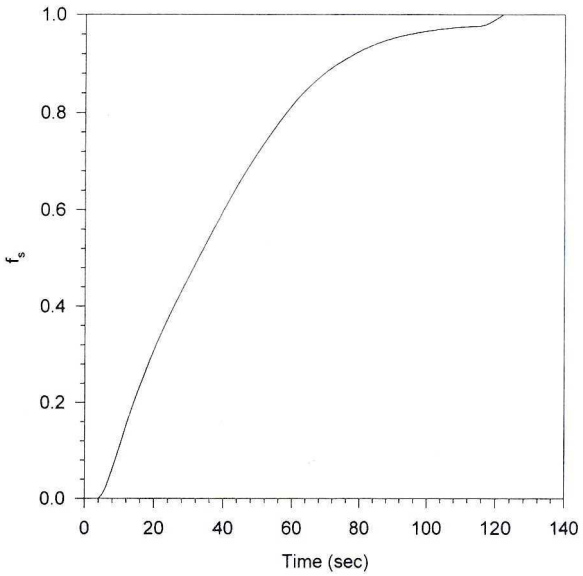

Fig. 5. Solid fraction evolution

4.4. Microscopic analysis

The microstructure and appearing phases of the alloy were identified using an optical microscope. It was possible to observe a dendrite equiaxed structure, with inter and intragranular carbides of the block morphology aligned in the inter-dendritic region. The observed carbides are of the M_6C type and its morphology is the typical for cobalt-based alloys with high content of Mo.

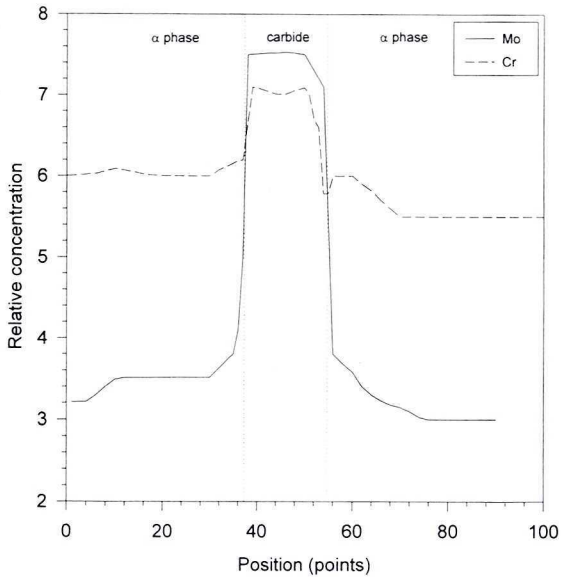

Fig. 6. Linear analysis across the interdendritic region (SEM)

In order to measure the segregation of main alloying elements, Cr and Mo, a linear analysis across the dendritic and interdendritic regions by using the scanning electron microscope was made. Figure 6 shows the results of such analysis. From this results it was possible to calculate the partition coefficients from the Eq. (9). However, it is necessary to note that the values of these solid/solid type partition coefficients are not the equilibrium values. This is due to very high cooling rates of solidification. Furthermore, the partition takes place on the solid/liquid interface and the back diffusion phenomenon in solid phases may be involved along with the formation of solute carbides or other complex solute compounds. The values of the partition coefficients are listed in table 4.

$$k_i = \frac{C_{i,1}}{C_{i,2}} \tag{9}$$

where k_i is the partition coefficient of the solute i; $C_{i,1}$ is the solute concentration in phase 1 and $C_{i,2}$ is the solute concentration in phase 2.

TABLE 4

Partition coefficients of the main alloying elements in the system C–Cr–Mo

Element	Mo	Cr
Partition coefficient (k_i) (interdendritic region/carbide	0.57	0.85
Partition coefficient (k_i) (dendrite/interdendritic region)	0.7	0.93

From these results is possible to observe that carbides are enriched in Cr and Mo with respect to the primary phase. It was found that Mo segregates more intensively than Cr. This is in agreement with other reported data [1].

5. Conclusions

This study has demonstrated that computer-aided cooling curve analysis is a practical optional method to evaluate the latent heat of solidification of the studied cobalt based alloy. Although, there was no other reported data for the latent heat of solidification for similar alloys for comparison, this method has been successfully tested with other alloys.

Applying presented method together with thermal analysis techniques, solidification kinetics study, chemical analysis and metallographic investigations, there is possible to obtain a complete understanding of the solidification process and, in this way, to correlate the thermal phenomena occurring during the process with the formation of microstructure. Finally, if the mathematical modeling of the solidification process of the alloy is to be performed, thermodynamic and thermophysical properties of the alloy are required to be known.

Acknowledgments

Authors are grateful for CONACYT (Grant No. 3075-A) and Polish State Scientific Committee (Grant No. 11.11.180.136) for financial support during this study.

REFERENCES

[1] D. Apelian, G. K. Sigworth, K. R. Whaler, Assessment of grain refinement and modification of Al–Si foundry alloys by thermal analysis, Trans. of the AFS, 459—469 (1984).

[2] L. Backerud, Recent developments in thermal analysis of aluminium casting alloys, 93rd Casting Congress, San Antonio, TX (1989).

[3] L. Backerud et al., Solidification characteristics of aluminium alloys, **1**, Des Plaines, ILL, AFS (1990).

[4] L. Backerud et al., Solidification characteristics of aluminium alloys, **2,** Des Plaines, ILL, AFS (1990).
[5] I. G. Chen, D. M. Stefanescu, Computer-aided differential thermal analysis of spheroidal and compact graphite cast irons, AFS Transactions **30,** 947—964 (1984).
[6] D. M. Stefanescu, G. Upadhya, D. Bandyopadhyay, Heat transfer-solidification kinetics modeling of solidification of castings, Metallurgical Transactions, **21 A,** 997—1005 (1990).
[7] L. Backerud, E. Krol, J. Tamminen, Solidification characteristics of aluminium alloys, Skanaluminium Universitetforlaget, Oslo, Norway 63—74 (1986).
[8] B. M. Bussian, W. Hardle, Robust smoothing applied to white norse and single outlier contaminated roman spectra, Appl. Spectrosc. **38,** 309—313 (1984).
[9] A. Savitsky, M. Golay, Smoothing and differentiation of data by simplified least squares procedures, Anal. Chem. **36** (8), 1627—1639 (1964).
[10] C. R. Brooks, Heat treatment, structure and properties of non-ferrous alloys, AFS, 229—251 (1982).
[11] S. Chu, J. Li, Z. Liu, Z. Shi, H. Fu, On morphologies, microsegregation and mechanical behavior of directionally solidified cobalt-base super alloy at medium cooling rate, Metallurgical and Materials Transactions **25 A,** 637—642 (1994).
[12] M. Rappaz, Ph. Thevoz, Solute diffusion model for equiaxed dendritic growth, Acta Metall. **35** (7), 1487—1497 (1987).
[13] M. Rappaz, Ph. Thevoz, Solute diffusion model for equiaxed dendritic growth, Acta Metall. **35** (12), 2929—2933 (1987).
[14] G. Chai, L. Backerud, T. Rolland, L. Arnberg, Dendrite coherency during equiaxed solidification in binary aluminium alloys, Metallurgical and Materials Transactions **26 A,** 965—970 (1995).

REVIEWED BY: DOC. DR HAB. INŻ. WALDEMAR WOŁCZYŃSKI

Received: 15 April 2000.